

Resonant Raman scattering in short-period $(\text{Si})_n/(\text{Ge})_m$ superlattices

F. Cerdeira,* M. I. Alonso, D. Niles, M. Garriga, and M. Cardona
*Max-Planck-Institut für Festkörperforschung, Heisenbergstrasse 1,
 D-7000 Stuttgart 80, Federal Republic of Germany*

E. Kasper and H. Kibbel
*Allgemeine Elektrizität-Gesellschaft Telefunken Research Center Ulm,
 D-7900 Ulm, Federal Republic of Germany*
 (Received 17 April 1989)

We have measured the resonant Raman efficiencies of different modes of $(\text{Si})_n/(\text{Ge})_m$ short-period superlattices as well as those of a $\text{Si}_{0.4}\text{Ge}_{0.6}$ random alloy in the range $1.8 \text{ eV} \leq \hbar\omega_L \leq 3.0 \text{ eV}$. The two peaks observed in the curves of Raman cross sections versus photon energy originate in extended (confined within the Ge layers) electronic states for the higher (lower) energy peak. These two types of optical transitions seem to merge as the layer thickness decreases. We attempt to explain these results on the basis of recent calculations of the electronic structure of these materials. As a byproduct we have obtained the absorption coefficients of our superlattices in the region below 3.1 eV.

The possibility of growing high-quality strained-layer superlattices made of ultrathin Si/Ge layers on Si, Ge, or $\text{Si}_{1-x}\text{Ge}_x$ substrates has been demonstrated by several authors.¹⁻³ Recent modulated reflectivity measurements⁴ have shown a richness of optical transitions which are attributed to folded and confined electronic states. Band calculations using diverse theoretical methods reproduce these results with varying degrees of success.⁵⁻⁹ These calculations also give the spatial extent of the electronic wave functions, thus allowing discrimination between states that are localized in either of the two types of layers, and those that are extended throughout the whole superlattice.

Although modulation spectroscopy is both sensitive and accurate for the determination of the energies at which optical transitions occur, it does not distinguish between localized and extended states. Resonant Raman scattering (RRS) is a complementary technique. Though it does not allow for accurate determination of transition energies, it provides information on localization by exploiting the modulation produced in the electronic states by the different types of phonons which appear in the superlattice spectrum.¹⁰ The latter can be either localized in the Ge or Si layers (optical modes) or extended through the whole structure (folded acoustic modes). The Raman cross section of each of these modes should have peaks when the frequency of the incident or scattered light coincides with that of electronic transitions originating in states which are modulated by that particular phonon and show no structure if the phonon and electronic states are localized in different layers. The usefulness of RRS to distinguish between localized and extended electronic states was first demonstrated for $\text{GaAs}/\text{Al}_x\text{Ga}_{1-x}\text{As}$ superlattices,¹¹ and was later used for other materials.¹⁰ In the present work we report the results of RRS experiments performed on short-period Si/Ge superlattices in the phonon energy range 1.8–3.0 eV. Our results show clear evidence of

direct optical transitions with different degree of localization.

The superlattices were grown by molecular-beam epitaxy (MBE) on a Si(001) substrate. Strain symmetrization was achieved by previously growing a thin (20 nm) Si-Ge alloy buffer layer of appropriate composition.^{1,2} Superlattices were grown on this buffer by alternating n monolayers of Si with m monolayers of Ge until a total thickness $d \approx 200 \text{ nm}$ was reached. In our experiments we used three superlattice samples: $(\text{Si})_4/(\text{Ge})_4$, $(\text{Si})_{12}/(\text{Ge})_8$, and $(\text{Si})_{10}/(\text{Ge})_{12}$. Raman measurements were performed in the configuration $z(x',x')\bar{z}$, where $x' = [1\bar{1}0]$, $y' = [110]$, and $z = [001]$ is the superlattice axis. The sample was kept at 100 K in a cold-finger liquid-nitrogen cryostat. Exciting radiation was obtained from discrete lines of argon, krypton, and He-Cd lasers as well as from the continuous emission of a dye laser with Rhodamine-6G and Coumarine-6 dyes.

A typical Raman spectrum is shown in the inset of Fig. 1, where peaks labeled *A*, *B*, *C*, *D*, and *E* correspond to folded LA modes (*A*), confined Ge LO (*B*), mixed alloy Si-Ge mode with interface mode (*C*), confined Si LO (*D*), and bulk Si mode (*E*) from the substrate. This identification is discussed in detail elsewhere.¹² A sample of bulk Si having the same orientation was mounted beside each superlattice for use as an intensity reference. The intensities of each Raman line of the superlattice were measured relative to that of the bulk Si sample as a function of laser energy. The Raman efficiencies thus obtained were corrected using the known¹³ cross section of pure Si and the absorption of the superlattice according to¹⁴

$$S^* = S[1 - \exp(-2ad)]/2a, \quad (1)$$

where S^* (S) is the measured (real) scattering efficiency, d is the thickness of the whole superlattice, and a is its absorption coefficient. The latter is obtained from the sub-

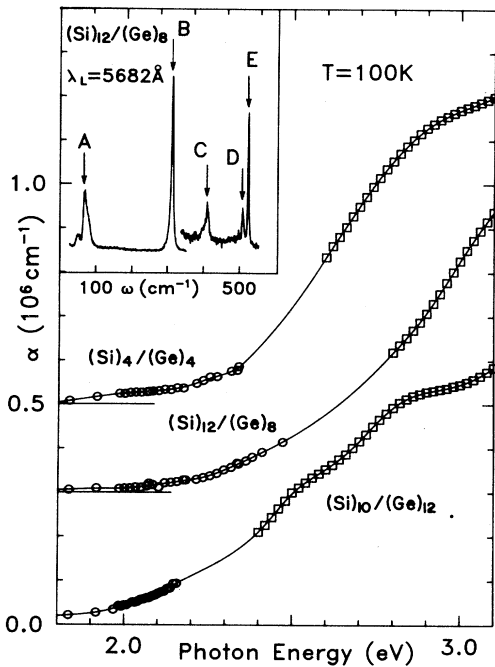


FIG. 1. Absorption coefficients of the $(\text{Si})_n/(\text{Ge})_m$ superlattices obtained by interpolating (solid line), Raman (open circles), and ellipsometric (open squares) data. The origin has been shifted in the upper two curves (indicated on the left-hand side) and the vertical scale is linear. Inset: A typical Raman spectrum.

strate Raman peak, whose intensity decreases as incoming and scattered light are absorbed in the film.¹⁵ The buffer layer absorption was neglected in the determination of α , since it is at least 1 order-of-magnitude thinner than the superlattice. This method of obtaining the absorption of the superlattice can be used up to $\hbar\omega_L \lesssim 2.4$ eV. Above this photon energy, the film becomes opaque and the substrate peak (E) disappears from the spectra. We had to turn to ellipsometric data to estimate the superlattice absorption for $\hbar\omega > 2.4$ eV. Unfortunately, the ellipsometric data could not be used for photon energies below ~ 2.6 eV because of strong oscillations produced by interference effects.¹⁶ Figure 1 shows the absorption coefficients used to correct the Raman measurements, obtained by performing a spline interpolation (solid line) between Raman (circles) and ellipsometric (squares) data.

The corrected Raman efficiencies of the superlattice modes corresponding to confined LO (filled and open circles) and folded LA (open triangles) modes are displayed in Fig. 2, where a solid line linking points (filled circles) corresponding to the confined Si modes was drawn as a guide for the eye. In the sample with the thickest Ge layers $[(\text{Si})_{10}/(\text{Ge})_{12}]$, two distinct resonant features are observed, centered at incident photon energies of approximately 2.25 and 2.9 eV. At the lowest of the two energies, the efficiency of the LO vibration localized in the Ge layers has a peak while the Si localized vibration does not. At $\hbar\omega_L \approx 2.9$ eV both of these modes exhibit maxima in their Raman efficiencies. The efficiency of the folded LA

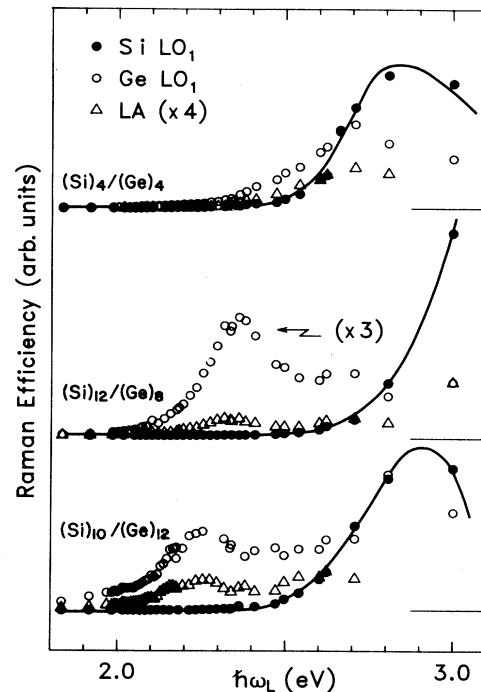


FIG. 2. Raman efficiency of confined LO and folded acoustic modes of $(\text{Si})_n/(\text{Ge})_m$ superlattices vs the energy of the incoming laser light ($\hbar\omega_L$).

modes, which propagate through the superlattice, exhibits weak maxima at or near both frequencies. This clearly means that the first resonance originates from optical transitions corresponding to electronic states confined in the Ge layers, while the second corresponds to extended electronic states. A similar pattern is exhibited by the $(\text{Si})_{12}/(\text{Ge})_8$ superlattice. The shift of both resonant maxima towards higher energies is easy to understand. The first peak should move this way because of greater confinement by a narrower Ge layer. The extended state, which stems from mixture of Si-like (higher energy) with Ge-like (lower energy) states, should also be at higher energy for the superlattice with the highest Si content (60% as opposed to 45% in the other two samples). Finally, in the $(\text{Si})_4/(\text{Ge})_4$ superlattice both states are so close in energy that the distinction between these two groups of states is blurred.

The results presented above show that two distinct groups of optical transitions contribute to the resonant Raman cross section of $(\text{Si})_n/(\text{Ge})_m$ ($n, m > 4$) superlattices. At lower photon energies the main contribution comes from transitions between electronic states strongly confined in the Ge layers. Extended electronic states are responsible for the peaks in the Raman efficiencies observed at higher energies ($\hbar\omega_L \gtrsim 2.8$ eV). When the layers become very thin these two peaks become very close in energy because of the increasing energy (due to increasing confinement) of the lower transitions, until they overlap for $n=m=4$.

In order to say more about the origin of these electronic states it is necessary to look into recent band calcula-

tions⁵⁻⁹ and make certain assumptions. It has been suggested^{4,6} that for ultrathin layers ($m = n \leq 4$), one should consider the superlattice as a new material rather than try to explain its electronic properties with bulk Ge and Si states appropriately modified by strain and confinement. In this spirit, a meaningful way to obtain insight into the electronic structure of the superlattices is to introduce the effects of structural distortions and folding of the band structure in a disordered alloy of the same composition.

In Fig. 3 we show the dependence of the Raman efficiency on incident laser frequency for a $\text{Si}_{0.4}\text{Ge}_{0.6}$ alloy. The three main optical vibrations of the alloy (Ge-Ge, Si-Ge, and Si-Si),¹⁷ show very similar dependences of their efficiencies versus $\hbar\omega_L$. At $\hbar\omega_L = 2.25$ eV, the cross section has a peak easily attributed to E_0 ($\Gamma_v \rightarrow \Gamma_c$) transitions. At $\hbar\omega_L \approx 2.7$ eV they have a second, more intense, peak known to originate in E_1 transitions¹⁸ ($L_v \rightarrow L_c$ and $\Lambda_v \rightarrow \Lambda_c$). The arrows in Fig. 3 indicate the position of these optical transitions obtained from reflectivity¹⁹ and ellipsometric²⁰ data. The E_0 resonance is much weaker than the E_1 peak, and the relative intensity of the first decreases as one progresses from Ge-Ge modes towards Si-Si modes. This could be due to greater localization of the predominantly Ge-like Γ wave functions around Ge atoms. The resonant behavior of the three alloy phonons is also slightly different near the E_1 and $E_1 + \Delta_1$ energies. A straightforward comparison of Figs. 2 and 3 [especially the bottom part of Fig. 2 corresponding to $(\text{Si})_{10}/(\text{Ge})_{12}$] might lead one to believe that the first resonance observed in the cross section of the $(\text{Si})_n/(\text{Ge})_m$ superlattices is due to E_0 transitions confined in the Ge layers, while the higher resonances are due to E_1 transitions which are not confined. The existence of a strong E_0 -type resonance in this energy region was also inferred from RRS (Ref. 21) and electroreflectance²² results in the related $\text{Si}/\text{Si}_{1-x}\text{Ge}_x$ strained-layer superlattices. Also, recent band calculations for $(\text{Si})_n/(\text{Ge})_n$ ($n = 2, 4, \text{ and } 6$) superlattices predict confined conduction-band states at Γ (Refs. 6-9) and extended ones at L , although the energies of the calculated $\Gamma_v \rightarrow \Gamma'_{2c}$ transitions are smaller than those at which the first resonance occurs in our $(\text{Si})_4/(\text{Ge})_4$ sample.⁵⁻⁹

In spite of the possibility of the above explanation for the results of Fig. 2, we believe our data is best explained by attributing E_1 character to the optical transitions involved in both peaks of the Raman cross sections of $(\text{Si})_n/(\text{Ge})_m$ superlattices. In the discussion that follows we shall pursue this explanation using the notation developed by Froyen, Wood, and Zunger⁵ for L -point electronic states. The first conduction-band states L_c of bulk Si and Ge give rise to two states²³ in the $(\text{Si})_n/(\text{Ge})_n$ superlattices, labeled L_{c1} and L_{c2} in order of increasing energy. Although these states appear as extended in Ref. 5 for $n \leq 6$, energetic considerations require that L_{c1} be more Ge like and L_{c2} more Si like, since in the limit of very thick superlattices these states should evolve into bulk Ge (L_{c1}) and Si (L_{c2}) L_c states. Furthermore, the center of mass of the $L_v \rightarrow L_{c1,2}$ transitions is calculated

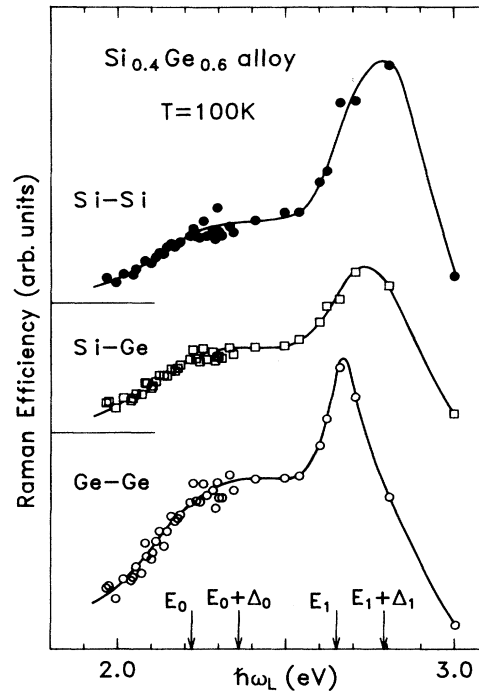


FIG. 3. Raman efficiency of the three main optical vibrations of a $\text{Si}_{0.4}\text{Ge}_{0.6}$ random alloy vs the frequency of the incoming laser.

(adding the local-density approximation correction)⁵ to occur at ~ 2.5 eV for $n = 4$, and the $L_{c2} - L_{c1}$ energy difference is small for this superlattice. Hence, we have two bands of E_1 transitions in the appropriate energy range, of which the lowest becomes more confined into the Ge layers as n becomes larger. This tendency was observed in ellipsometric measurements of short-period GaAs/AlAs superlattices.¹⁶ Also, a splitting of the E_1 transitions into several components ranging from 2.4 to 3.3 eV has been reported in Ref. 24 for $(\text{Si})_4/(\text{Ge})_4$ superlattices. The much larger oscillator strength expected for E_1 vs E_0 transitions favors this explanation over the (E_0, E_1) assignment previously discussed. Within this picture E_0 transitions would not be observed since they are weaker and occur at lower energy. However, we must keep in mind that these short-period superlattices are new materials in their own right and that explanations of their electronic structure in terms of bulk Si or Ge states might not be appropriate. Calculations including the whole Λ axis (as opposed to just the L point) as well as more experimental data are needed in order to make more definitive assignments.

We are grateful to M. Siemers for his expert help with dye lasers. H. Hirt and P. Wurster are also thanked for efficient technical help. Thanks are also due to G. Abstreiter for illuminating discussions.

- *Permanent address: Instituto de Física, Universidade Estadual de Campinas, 13081 Campinas, São Paulo, Brazil.
- ¹E. Kasper, H. J. Herzog, H. Dämbkes, and G. Abstreiter, in *Layered Structures and Epitaxy*, edited by J. M. Gibson, G. C. Osbourn, and R. M. Tromp, Materials Research Society Symposia Proceedings, Vol. 56 (Materials Research Society Pittsburgh, PA, 1986), p. 347.
- ²E. Kasper, H. Kibbel, H. Jorke, H. Brugger, E. Friess, and G. Abstreiter, *Phys. Rev. B* **38**, 3599 (1988).
- ³J. Bevk, A. Ourmazd, L. C. Feldman, T. P. Pearsall, J. M. Bonar, B. A. Davison, and J. P. Mannaerts, *Appl. Phys. Lett.* **50**, 760 (1987).
- ⁴T. P. Pearsall, J. Bevk, L. C. Feldman, J. M. Bonar, J. P. Mannaerts, and A. Ourmazd, *Phys. Rev. Lett.* **58**, 729 (1987).
- ⁵S. Froyen, D. M. Wood, and A. Zunger, *Phys. Rev. B* **36**, 4547 (1987); **37**, 6893 (1988).
- ⁶L. Brey and C. Tejedor, *Phys. Rev. Lett.* **59**, 1022 (1987).
- ⁷M. S. Hybertsen and M. Schlüter, *Phys. Rev. B* **36**, 9683 (1987).
- ⁸K. B. Wong, M. Jaros, I. Morrison, and J. P. Hagon, *Phys. Rev. Lett.* **60**, 2221 (1988).
- ⁹S. Satpathy, R. M. Martin, and C. G. Van de Walle, *Phys. Rev. B* **38**, 13237 (1988).
- ¹⁰For a recent review of the subject, see B. Jusserand and M. Cardona, in *Light Scattering in Solids V*, edited by M. Cardona and G. Güntherodt (Springer-Verlag, Heidelberg, 1989), p. 49.
- ¹¹J. E. Zucker, A. Pinczuk, D. S. Chemla, A. Gossard, and W. Wiegmann, *Phys. Rev. B* **29**, 7065 (1984).
- ¹²M. I. Alonso, F. Cerdeira, D. Nilas, M. Cardona, E. Kasper, and H. Kibbel (unpublished).
- ¹³A. Compaan and H. J. Trodahl, *Phys. Rev. B* **29**, 793 (1984).
- ¹⁴M. Cardona, in *Light Scattering in Solids II*, edited by M. Cardona and G. Güntherodt (Springer-Verlag, Heidelberg, 1982), p. 40.
- ¹⁵F. Cerdeira, A. Pinczuk, J. C. Bean, B. Batlogg, and B. A. Wilson, *J. Vac. Sci. Technol. B* **3**, 600 (1985).
- ¹⁶M. Garriga, M. Cardona, N. E. Christensen, P. Lautenschlager, T. Isu, and K. Ploog, *Phys. Rev. B* **36**, 3254 (1987).
- ¹⁷D. W. Feldman, M. Ashkin, and J. H. Parker, Jr., *Phys. Rev. Lett.* **17**, 1209 (1966).
- ¹⁸M. A. Renucci, J. B. Renucci, and M. Cardona, in *Proceedings of the Conference on Light Scattering in Solids*, edited by M. Balkanski (Flammarion, Paris, 1971), p. 326.
- ¹⁹J. S. Kline, F. H. Pollak, and M. Cardona, *Helv. Phys. Acta* **41**, 968 (1968).
- ²⁰J. Humlíček, M. Garriga, M. I. Alonso, and M. Cardona, *J. Appl. Phys.* **65**, 2827 (1989).
- ²¹F. Cerdeira, A. Pinczuk, and J. C. Bean, *Phys. Rev. B* **31**, 1202 (1985).
- ²²T. P. Pearsall, F. H. Pollak, J. C. Bean, and R. Hull, *Phys. Rev. B* **33**, 6821 (1986).
- ²³The further splitting that occurs in even- n superlattices due to their orthorhombic symmetry is not important to our discussion.
- ²⁴T. P. Pearsall, J. Bevk, J. C. Bean, J. Bonar, J. P. Mannaerts, and A. Ourmazd, *Phys. Rev. B* **39**, 3741 (1989).